An Arrhythmic Mutation E7K Facilitates TRPM4 Channel Activation via Enhanced PIP$_2$ Interaction

Yaopeng Hu [1,*]**, Qin Li** [2]**, Lin-Hai Kurahara** [3]**, Narumi Shioi** [4]**, Keizo Hiraishi** [3]**, Takayuki Fujita** [1]**, Xin Zhu** [2] **and Ryuji Inoue** [1,*]

1   Department of Physiology, School of Medicine, Fukuoka University, Fukuoka 814-0180, Japan; fujitaka@fukuoka-u.ac.jp
2   Biomedical Information Engineering Lab, The University of Aizu, Aizu-Wakamatsu 965-8580, Japan; aasynch@gmail.com (Q.L.); zhuxin@u-aizu.ac.jp (X.Z.)
3   Department of Cardiovascular Physiology, Faculty of Medicine, Kagawa University, Kagawa 761-0793, Japan; hailin@med.kagawa-u.ac.jp (L.-H.K.); kzohiraishi@med.kagawa-u.ac.jp (K.H.)
4   Department of Chemistry, Faculty of Science, Fukuoka University, Fukuoka 814-0180, Japan; anarumi@fukuoka-u.ac.jp
*   Correspondence: huyaopeng@fukuoka-u.ac.jp (Y.H.); inouery@fukuoka-u.ac.jp (R.I.)

Abstract: A Ca^{2+}-activated monovalent cation-selective TRPM4 channel is abundantly expressed in the heart. Recently, a single gain-of-function mutation identified in the distal N-terminus of the human TRPM4 channel (Glu^5 to Lys^5; E7K) was found to be arrhythmogenic because of enhanced cell membrane expression. In this study, we conducted detailed analyses of this mutant channel from more functional aspects, in comparison with its wild type (WT). In an expression system, intracellular application of a short soluble PIP$_2$ (diC$_8$PIP$_2$) restored the single-channel activities of both WT and E7K, which had quickly faded after membrane excision. The potency (K$_d$) of diC$_8$PIP$_2$ for this recovery was stronger in E7K than its WT (1.44 vs. 2.40 μM). FRET-based PIP$_2$ measurements combined with the *Danio rerio* voltage-sensing phosphatase (DrVSP) and patch clamping revealed that lowering the endogenous PIP$_2$ level by DrVSP activation reduced the TRPM4 channel activity. This effect was less prominent in E7K than its WT (apparent K$_d$ values estimated from DrVSP-mediated PIP$_2$ depletion: 0.97 and 1.06 μM, respectively), being associated with the differential PIP$_2$-mediated modulation of voltage dependence. Moreover, intracellular perfusion of short N-terminal polypeptides containing either the 'WT' or 'E7K' sequences respectively attenuated the TRPM4 channel activation at whole-cell and single-channel levels, but in both configurations, the E7K polypeptide exerted greater inhibitory effects. These results collectively suggest that N-terminal interaction with endogenous PIP$_2$ is essential for the TRPM4 channel to function, the extent of which may be abnormally strengthened by the E7K mutation through modulating voltage-dependent activation. The altered PIP$_2$ interaction may account for the arrhythmogenic potential of this mutation.

Keywords: arrhythmogenicity; PIP$_2$; TRP channel

1. Introduction

Despite steady advancements in prevention and treatment in the past few decades, cardiac arrhythmias remain among the leading causes of mortality in developed countries [1]. Thus, comprehensive understanding their pathogenesis continues to be an important goal with the highest priority. Recently, transient receptor potential (TRP) channels have drawn increasing attention because of their active involvement in cardiac pathophysiology including arrhythmias [2,3]. A notable example is the melastatin subfamily member TRPM4, which functions as a Ca^{2+}-activated monovalent cation-selective cation channel [4]. It has been suggested that TRPM4 contributes to the prolongation of action potential (AP) and generation of early afterdepolarization (EAD) [5]. In clinical studies, the N-terminal mutation c.19G → A in the TRPM4 gene (i.e., p.7E → K) was found in a few pedigrees of

patients manifesting progressive conduction blocks and was associated with sudden death. This mutation was shown to increase the cell-surface expression of the TRPM4 channel protein via impaired SUMOylation in vitro, and may thus cause a depolarizing shift of the resting membrane potential [6]. This would in turn facilitate the inactivation of the voltage-dependent Na^+ channels and presumably induce cell death, which may account for the observed fibrotic degeneration of Purkinje fibers, ultimately leading to conduction failures [7].

An increasing number of studies support the importance of protein–lipid interactions in ion channel regulation [8]. In particular, PIP_2 is thought to be essential for the normal activities of many ion channels and transporters in the plasma membrane [9]. In the heart, beat-to-beat activation of ion channels is finely controlled by the autonomic nerves and strongly influenced by cardioactive peptides/hormones, many of which act through the stimulation of G protein-coupled receptors (GPCRs), which are tightly linked to PIP_2 metabolism. In some animal models of chronic heart failure in which β-adrenergic and angiotensin II receptors were overactive [10], the membrane PIP_2 content was found to be decreased along with an altered PIP_2 metabolism [11]. These facts raise the possibility that disrupted PIP_2 metabolism under sustained neurohormonal stresses may affect the balance of ionic flows across the cardiomyocyte membrane, thereby predisposing individuals to arrhythmias.

It has been shown that PIP_2 strongly enhances the wild-type TRPM4 channel activity and partially rescues it from desensitization [12,13]. However, these studies simply depleted endogenous PIP_2 by pharmacological/biochemical interventions or exogenously applied artificial PIP_2 to investigate their steady-state effects on the channel. It should, however, be noted that endogenous PIP_2 levels fluctuate in conjunction with the GPCR-dependent phospholipase C (PLC) activity, which is subject to the activities of autonomic nerves and other bioactive agents. This fact necessitates a reevaluation of the dynamic influence of PIP_2 on TRPM4 channel activity under the conditions that enable it to control the membrane PIP_2 level in fast and quantitative manners.

To accomplish this goal, we performed real-time PIP_2 monitoring with FRET sensors in combination with the *Danio rerio* voltage-sensing phosphatase (DrVSP), which allowed us to manipulate the endogenous PIP_2 level in a graded manner [14]. The data obtained by this methodological approach suggest that, compared with its wild type (WT), the E7K mutation renders the voltage dependence of the TRPM4 channel to be much less susceptible to PIP_2 depletion, thereby enhancing the channel activity.

2. Materials and Methods

2.1. Cell Culture and Gene Transfection

Human embryonic kidney cells 293 (HEK293; ATCC, Manassas, VA, USA) were cultured in Dulbecco's modified Eagle medium (DMEM) and supplemented with 10% FBS and antibiotics under 100% humidified, 5% CO_2-gassed conditions. For transfection, the near-confluent cells were dissociated by short trypsin treatment and gentle trituration with a large-bored Pasteur pipette, and replated on cover slips that were precoated with poly L-lysin (30 μg/mL). About 12 h later, the coverslips were incubated in a transfection medium (either DMEM or $Opti^{TM}$) containing 1 μg pcI-neo vector that encodes the CDS of the TRPM4b gene or that of the E7K mutant, 1 μg DrVSP-encoding pIRES-eGFP vector and each of 0.3 μg plasmids encoding CFPmse-PHd and YFPmse-PHd (see below) with the aid of transfection agents Superfect (Qiagen, Hilden, Germany) or lipofectatmine 2000^{TM} (Invitrogen, Waltham, MA, USA). The protocol used for the transfection followed the manufactures' instructions. Electrophysiological measurements were performed at room temperature 36–48 h after the transfection. The human TRPM4b cDNA (Gene ACC. No: AF497623) inserted into the pcDNA4TO-Flag vector was originally provided by Professors J.-P. Kinet (Beth Israel Deaconess Medical Center and Harvard Medical School, Boston, MA, USA) and P. Launay (INSERM, Paris, France) and subcloned into the pcI-neo vector. Enhanced FRET pairs combined with the $PI(4,5)P_2$ sensor molecules, CFPmse-PHd

and YFPmse-PHd, were synthesized by fusing CFPmse and YFPmse to the pleckstrin homology domain of PLCδ1 [15], as performed previously [16].

2.2. Solution

The standard external solution contained (in mM): 140 NaCl, 5 KCl, 1 $CaCl_2$, 1.2 $MgCl_2$, 10 HEPES, and 10 glucose (pH 7.4, adjusted with Tris base). The pipette solution for the whole-cell and inside-out (I/O) recordings contained (in mM): 120 Cs-aspartate, 20 CsCl, 2 $MgCl_2$, 5 EGTA, 10 Hepes, 2 ATP, 0.1 GTP, and 10 glucose (adjusted to pH 7.2 with Tris base), to which an optimal amount of Ca^{2+} was added to give a desired $[Ca^{2+}]$ value. The $[Ca^{2+}]$ value of the pipette solution was calculated by using a custom-written program based on Fabiato and Fabiato's algorithm written in Visual Basic with the enthalpic and ionic strength corrections of the association constants [17].

2.3. Electrophysiology

The whole-cell and I/O modes of the patch-clamp technique were employed for the membrane current recording. Electrodes with the input resistance of 4–6 MΩ (when filled with internal solution) were made from 1.5-mm borosilicate glass capillaries (Sutter Instrument), and connected to the headstage of a low-noise, high-impedance patch-clamp amplifier (EPC10, HEKA Elektronik, Ludwigshafen, Germany). The amplifier was controlled by the automated multichannel data acquisition software 'Patchmaster' (HEKA, Ludwigshafen, Germany). In total, >60% of series resistance was electronically compensated. For continuous monitoring, current and voltage signals were sampled via the PowerLab data acquisition system (AD Instruments, Sydney, Australia) and subjected to subsequent offline analyses. For kinetic analyses and illustrations, data exported in the matlab or text formats were processed by the commercial data analysis software Origin v.9.1 (LightStone, Tokyo, Japan), Clampfit v.10 (Axon Instruments, Foster City, CA, USA), Excel 2012, and KaleidaGraph v.4 (Hulinks, Tokyo, Japan). To activate DrVSP, depolarizing step pulses (from the holding potential of −60 mV to 120 mV) of varying durations were applied every 120 s. The ratio of the inward currents after (I_{post}) to before (I_{pre}) DrVSP activation was used to calculate the degree of DrVSP-mediated inhibition according to the equation: $1.0 - I_{post}/I_{pre}$.

2.4. FRET Measurement

The method used for FRET measurement was essentially the same as described previously [16]. In brief, fluorescence emissions from voltage-clamped cells were obtained via a high-sensitivity sCMOS camera (Andor Neo; Andor Technology) equipped to a microscope (IX71; Nikon, Tokyo, Japan). Excitation lights filtered at 430 ± 10 and 504 ± 12 nm, respectively, were alternately shone by a computer-controlled high-speed wavelength-switching light source (Lambda DG-4, Sutter Instrument Co., Novato, CA, USA). Epifluorescence was first prefiltered through a multiband dichroic mirror (449–483 and 530–569 nm) contained in the microscope, and then separated and filtered in a beam splitter (Dual-View2; Photometrics) at 464 ± 23 nm (for donor fluorescence) and 542 ± 27 nm (for acceptor fluorescence). The duration of the camera exposure was confined to 250 ms within the 300-ms period of illumination for each excitation wavelength. Captured images were digitized as 16-bit, 512×512 pixels using the imaging software 'MetaMorph v.7.7'. Averaged intensities from the whole-cell region were also calculated by this software to obtain the FRET. FRET and electrophysiological measurements were synchronized by a brief trigger output from the PowerLab (AD Instruments, Sydney, Australia) to the excitation light shutter.

To specify each observed fluorescence (F), the descriptor $F_{X(Y)}$ is used in this paper, where X and Y denote the emission and excitation filter settings, respectively. Specifically, 'X' denotes either the emission at 464 nm from the donor (CFPmse-PHd) or that at 542 nm from the acceptor (YFPmse-PHd). 'Y' denotes the filter settings used to excite the donor (at 430 nm) and acceptor (at 504 nm), thus dubbed 'D' and 'A', respectively. The FRET ratio (FR) was calculated according to the '3-cube' method [18] instead of

the raw values: $FR = (F_{542(D)} - RD1 \times F_{464(D)})/RA \times (F_{542(A)} - RD2 \times F_{542(D)})$, where $RD1 = F0_{542(D)}/F0_{464(D)}$, $RD2 = F0_{542(A)}/F0_{464(D)}$, and $RA = F0_{542(D)}/F0_{542(A)}$. The constants RD1, RD2, and RA were predetermined by the fluorescence (F0) from single cells expressing either the empty donor (CFPmse) or the acceptor (YFPmse). Background fluorescence, measured from non-transfected cells by each filter setting, was corrected by subtraction.

2.5. Statistical Evaluation

All experimental data are expressed as the mean $\pm$ SEM. Statistical significance ($p < 0.05$) was evaluated by the Student's *t*-test or ANOVA with Tukey's or Dunnett's post hoc tests for single or multiple comparisons, respectively.

3. Results

3.1. DiC$_8$-PIP$_2$ More Potently Reactivates E7K Than WT-TRPM4 Channels

First, to confirm the previous finding that PI(4,5)P$_2$ is essential for TRPM4 channel activity [12,13], and to explore whether there is any difference in PIP$_2$ sensitivity between its WT and E7K mutant, we performed single-channel recordings of TRPM4 channels heterologously expressed in HEK293 cells. Both the WT- and E7K-TRPM4 channels underwent rapid desensitization/rundown upon membrane excision into a 300 μM Ca^{2+}-containing bathing solution. The subsequent application of a water-soluble short form of PIP$_2$, diC$_8$-PI(4,5)P$_2$ (5 μM) quickly restored the channel activity in both channels. (Figure 1A). To quantify these effects, we applied a broader concentration range of diC$_8$-PIP$_2$ (0.2–20 μM) in an incremental manner (Figure 1B). The extent of reactivation (see the Figure 1 legend) was well described by a Hill-type equation with apparent EC$_{50}$ values of 2.40 $\pm$ 0.23 μM ($n = 5$) and 1.44 $\pm$ 0.20 μM ($n = 5$) for the WT- and E7K-TRPM4 channels, respectively (Figure 1C). These results indicate that the E7K mutant is more potently reactivated by diC$_8$-PIP$_2$ than its WT.

3.2. Simultaneous Measurements of Endogenous PI(4,5)P$_2$ and TRPM4 Channel Activity

To explore the significance of the above finding in a more physiological context, we next investigated the functional correlation between the magnitude of the whole-cell TRPM4 current and endogenous PIP$_2$ level, on the basis of the same approach as adopted previously [16]. Specifically, depolarizing pulses were applied to activate DrVSP, and thereby dephosphorylate PIP$_2$, in the cell membrane. To monitor the endogenous PIP$_2$ level, we employed CFPmse-PHd and YFPmse-PHd as a FRET donor/acceptor pair. Under unstimulated conditions, this pair is presumed to localize mostly in close vicinity at the inner cell membrane, thereby producing significant FRET, while after PIP$_2$ depletion, it is expected to dissociate from the membrane to decrease FRET. In addition, the whole-cell TRPM4 current was induced by the intracellular infusion of a moderate concentration of Ca^{2+} (1 μM) via sharp patch electrodes in order to minimize the time-dependent desensitization/rundown, as performed previously [19]. Figure 2A demonstrates the typical recordings of the fluorescence intensities of CFPmse-PHd and YFPmse-PHd in response to a brief depolarizing pulse from -60 mV to $+120$ mV. Immediately after DrVSP activation by the depolarizing pulse (Figure 2Aa), the acceptor fluorescence by donor excitation ($F_{542(D)}$) decreased (Figure 2Ad), while the donor fluorescence by donor excitation ($F_{464(D)}$) increased (Figure 2Ab), and then both recovered slowly to the original levels. In contrast, the acceptor fluorescence by acceptor excitation ($F_{542(A)}$) remained almost constant before and after DrVSP activation (Figure 2Ac). The reciprocal changes in $F_{542(D)}$ and $F_{464(D)}$ suggest that a substantial decrease occurred in the efficiency of FRET from CFPmse-PHd to YFPmse-PHd upon the depolarization-induced PIP$_2$ depletion. The slow recovery of the fluorescence intensities most likely reflects the replenishment of membrane PIP$_2$ by PIP-5-kinase [20]. After the correction of nonspecific fluorescence changes by the 3-cube method (see the Materials and Methods Section) [16,18], the value of the FRET ratio (FR), which would faithfully reflect the dynamic change of membrane PIP$_2$ level, showed a more prominent decrease and recovery over time (Figure 2Bc). The time course of this FR change exactly coincided with that of the TRPM4 current that was simultaneously recorded (Figure 2Bc).

This temporal coincidence strongly supports that the TRPM4 channel activity is closely corelated with the endogenous PIP$_2$ level.
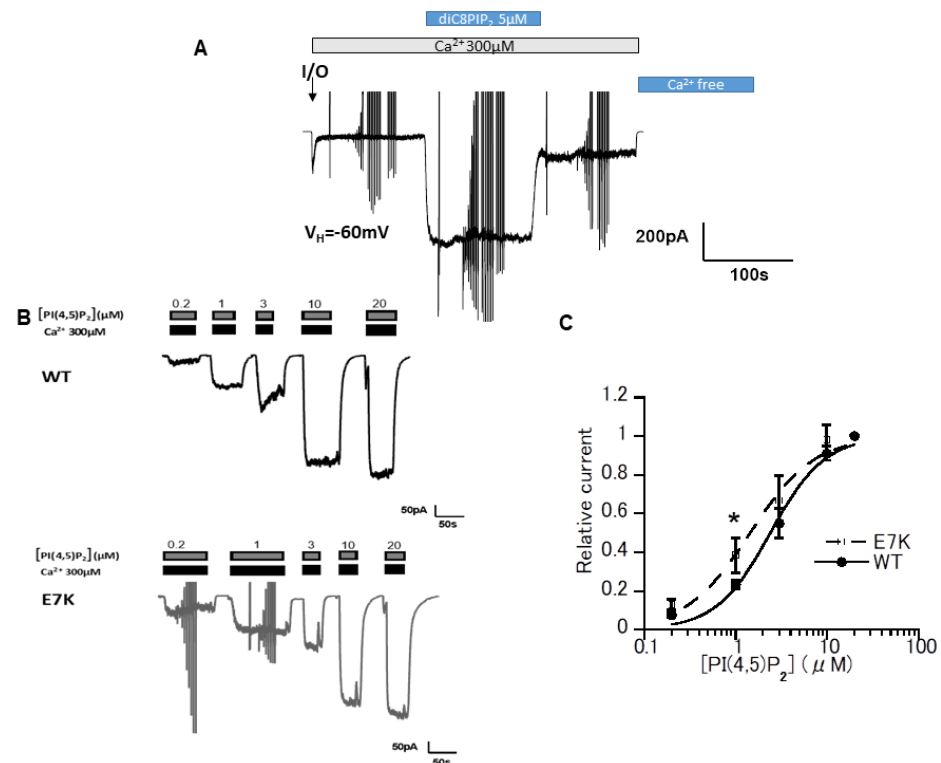

Figure 1. E7K mutant presented a higher PI(4,5)P$_2$ sensitivity than the wild-type (WT)-TRPM4 channel. (**A**) In the inside-out patch configuration and after the fast rundown, diC$_8$-PI(4,5)P$_2$ (5 µM) restored TRPM4 channel activity over its initial magnitude. Vertical deflections reflect ramp- or step pulse-induced currents. (**B**) Representative data from two inside-out patch membranes (WT and E7K) demonstrating the dose-dependent reactivation of TRPM4 channels in response to various concentrations of diC$_8$-PI(4,5)P$_2$. (**C**) The degree of reactivation by diC$_8$-PI(4,5)P$_2$ (relative current) is defined as $(I_{[x]} - I_{[post-desens]})/(I_{[20 \mu M\ diC8-PIP2]} - I_{[post-desens]})$, where $I_{[x]}$ and I respectively denote the amplitudes of TRPM4 currents reactivated by given ('X' µM) and maximal (20 µM) concentrations of diC$_8$-PI(4,5)P$_2$, and $I_{[post-desens]}$ is that of the basal TRPM4 current after desensitization to 300 µM Ca^{2+} [13]. Averaged concentration-response curves for the TRPM4 channel reactivation by diC$_8$-PI(4,5)P$_2$ are fitted by the Hill-type equation: $1/(1 + (EC_{50}/[diC_8PIP_2])^n$. It gives EC$_{50}$ values of 2.40 ± 0.23 µM and 1.44 ± 0.20 µM; Hill coefficient (*n*) values of 1.5 and 1.2 for WT and E7K, respectively. * $p < 0.05$ with ANOVA followed by Tukey's post hoc tests (*n* = 5).

3.3. Differential PIP$_2$ Sensitivities of WT and E7K-Mutant TRPM4 Channels

In the next step, we further questioned whether WT- and E7K-TRPM4 channels have differential sensitivities to the endogenous PIP$_2$ level. Depolarizing pulses of incremental durations (300–2000 ms) were applied to activate DrVSP and deplete membrane PIP$_2$ in a graded fashion [21]. As demonstrated in Figure 3A, prolonging the pulse duration progressively decreased both the FR value and the whole-cell TRPM4 current amplitude (I$_m$). Notably, even though there was no difference in the maximum inhibition of current amplitude, the degree of TRPM4 current inhibition by a given duration of depolarization (or value of FR) was smaller in E7K-mutant channels than in the WT-channels (open vs. filled circles in Figure 3B). After converting the FR value into the endogenous PIP$_2$ level (see the Figure 3 legend), the relationship between the TRPM4 current inhibition and endogenous PIP$_2$ level demonstrated a higher PIP$_2$ sensitivity of E7K-mutant channels than the WT-TRPM4 channels (Figure 3C), especially near the range of K$_d$ values. Moreover, the recovery from the inhibition was significantly faster in E7K- than WT-TRPM4 channels

(Figure 3Da); the time constants of recovery were 13.71 ± 4.24 s and 17.56 ± 5.29 s for E7K and WT, respectively. These observations raise the idea that the E7K mutation may render the TRPM4 channel more tightly bound to endogenous PIP$_2$, thereby stabilizing its activity.
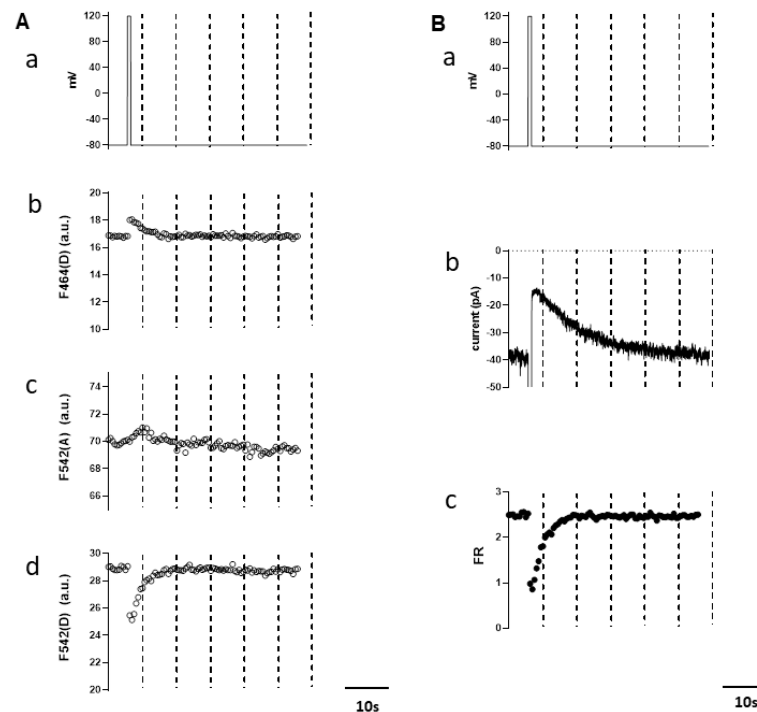

Figure 2. Simultaneous measurement of TRPM4 current and endogenous PI(4,5)P$_2$ level. Typical example of DrVSP-mediated TRPM4 currents' change induced by the depolarization and the corresponding FRET changes. (**A**) A 1-s-long depolarizing pulse (from -60 to 120 mV; (a)) and the changes of the fluorescence intensities (in a.u.) recorded through three different filter settings, F$_{464(D)}$ (b), F$_{542(A)}$ (c), and F$_{542(D)}$ (d). (**B**) A 1-s-long depolarizing pulse (a), the time course of inward TRPM4 current inhibition during the depolarization (b), and that of the FRET ratio (FR) (c). The value of FR is calculated by the 3-cube method (see the Materials and Methods Section and text).

3.4. PIP$_2$ Depletion Only Modestly Affects the Voltage-Dependent Activation of E7K Mutant Because of Its Higher PIP$_2$ Affinity

It is well known that TRPM4 channels are positively regulated by the membrane potential. Although the mechanism of actions remains unclear, application of diC$_8$-PIP$_2$ was found to cause a remarkable leftward shift in the voltage dependence of strongly desensitized TRPM4 channels after membrane excision into mM concentrations of Ca^{2+} [12]. We therefore examined how transient depletion of endogenous PIP$_2$ by DrVSP activation affects the voltage dependence of whole-cell WT- and E7K-TRPM4 currents under the milder conditions where desensitization is much less evident, as in Figures 2 and 3. To make the time required to evaluate the voltage dependence as short as possible, we employed a dual-ramp protocol consisting of 1-s-long ascending and descending voltage ramps (-100–200 mV), between which a depolarizing step pulse to $+120$ mV was inserted (top panel in Figure 4A). The voltage ramps spanned the almost full range of the TRPM4 channel activation, and the 2-s depolarization was sufficient to maximally lower the membrane PIP$_2$ level (bottom panel in Figure 4A). In the absence of DrVSP, there was no discernible decrease of the current amplitude during depolarization to $+120$ mV and the following descending ramp in either WT- or E7K-mutant TRPM4 channels (data not shown). By this protocol, we could characterize the differences in voltage dependence before and after PIP$_2$ depletion between WT- and E7K-TRPM4 channels.
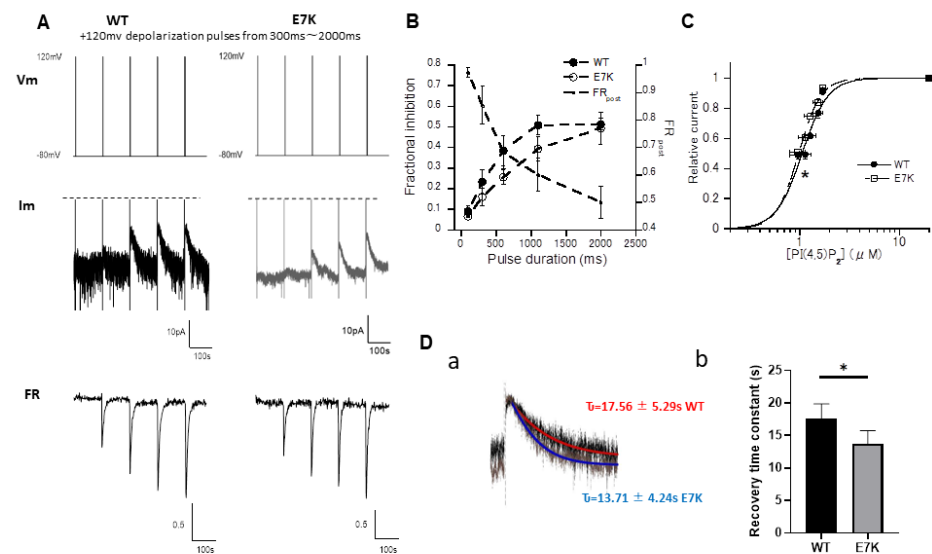
Figure 3. Quantitative relationships between endogenous PIP$_2$ level and whole-cell TRPM4 current amplitude for WT and E7K mutant. (**A**) Graded depletion of endogenous PI(4,5)P$_2$ was attained by applying a set of depolarizing pulses of incremental duration (300–2000 ms; from −60 to 120 mV). To minimize time-dependent changes due to desensitization, a relatively low concentration of Ca^{2+} (1 μM) was included in the pipette to induce TRPM4 currents under the whole-cell conditions. The tree panels in the figure denote the simultaneously recorded whole-cell TRPM4 current (I$_m$) and concomitant FRET ratio (FR) in response to depolarizing pulses of incremental duration (300–2000 ms; V$_m$). Prolongation of depolarizing pulses resulted in the progressive inhibition of whole-cell TRPM4 currents, the extent of which was greater for WT than E7K, despite the same degree of FR decrease (i.e., PIP$_2$ depletion). (**B**) Duration-dependent inhibition of the whole-cell TRPM4 current by depolarization-induced PIP$_2$ depletion for WT and E7K (open vs. filled circles). The duration-dependent inhibition is defined by using the ratio of TRPM4 current amplitudes before (I$_{pre}$) and after (I$_{post}$) each depolarization according to the formula: fractional inhibition = 1 − I$_{post}$/I$_{pre}$, which is plotted against the pulse duration. FR change is also displayed together (dashed curve). (**C**) The relationships between endogenous PIP$_2$ concentration and WT- or E7K-TRPM4 channel activity (normalized whole-cell current amplitude). Endogenous PIP$_2$ concentration was estimated from the FR value after the previous study [16] according to the formula: $\frac{FR}{FR_{max}} \approx F^2 = \left\{ 1 / \left(1 + \frac{K_d}{[PI(4,5)P_2]} \right) \right\}^2$, where FR_{max} was determined from PIP5K-overexpressing cells as a 1.2-fold higher value than that evaluated from the control cells [16]. The apparent K$_d$ values of PI(4,5)P$_2$ binding to WT- TRPM4 channels and E7K-mutant TRPM4 channels determined by this method were 1.06 ± 0.05 μM and 0.97 ± 0.02 μM, respectively. *: $p < 0.05$ with ANOVA followed by Tukey's post hoc tests ($n = 5$). (**D**) Time courses of the whole-cell TRPM4 currents recovering from depolarization-induced, DrVSP-mediated inhibition for WT (red curve in a) and E7K (blue curve in a). The time constant of recovery (τ) was determined by mono-exponential fitting, which resulted in values of 17.56 ± 5.29 and 13.71 ± 4.24 s for WT and E7K, respectively (b). *: $p < 0.05$ with unpaired t-test, respectively ($n = 5$).
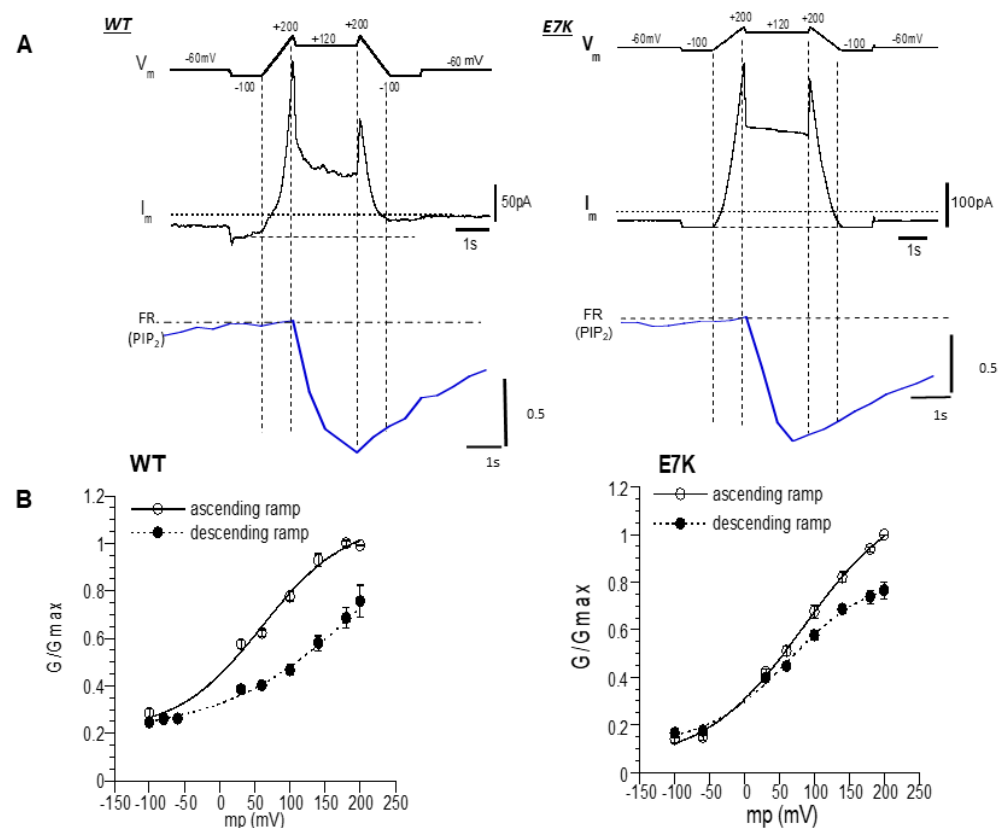
Figure 4. Different voltage dependence between the WT-TRPM4 channel and E7K-mutant TRPM4 channel after VSP-induced PIP_2 depletion. (**A**) The left and right three panels show data from WT and E7K, respectively. Top panel (V_m): a dual-ramp protocol consisting of an ascending ramp of 1 s, sustained depolarization at +120 mV for 2 s, and a descending ramp of 1 s. The ramps spanned between −100 and 200 mV. Middle and bottom panels (I_m and FR): representative simultaneous recordings of membrane currents and FRET ratios (which represent the endogenous PIP_2 level) during V_m changes. (**B**) Chord conductance (G)-V_m relationships for WT- and E7K-mutant TRPM4 channels before (open circles) and after (filled circles) DrVSP-mediated PIP_2 depletion. The values of G/G_{max} were calculated from the data as shown in A, and the G_{max} was taken as the maximal G value at 200 mV of the ascending ramp. After PIP_2 depletion, the voltage dependence of the WT-TRPM4 channel was remarkably rightward shifted. In contrast, this shift was only marginal for E7K mutant, especially around the resting membrane potential. After fitting of these G-V data to the Boltzmann equation: $G/G_{max} = G_0/G_{max} + (G_{max} − G_0)/(1 + \exp((V_{0.5} − V_m)/s)$ (V_m, $V_{0.5}$, s: membrane potential, half-maximal activation voltage, slope factor, respectively), the $V_{0.5}$ values before and after DrVSP activation: 62.07 ± 7.32 and 83.31 ± 9.53 vs. 59.63 ± 10.79 and 219.84 ± 75.37; and the s values before and after DrVSP activation (mV): 58.79 ± 11.46 mV and 70.45 ± 12.69 mV vs. 60.04 ± 18.52 mV and 101.58 ± 26.29, were obtained for the E7K-mutant and WT-TRPM4 channels, respectively (*n* = 8). Note that in both WT and E7K, there appeared to be a substantial non-voltage-dependent component (G_0/G_{max}) at very negative potentials, which may reflect incomplete PIP_2 depletion by a 2-s depolarization to +120 mV.

As illustrated in Figure 4B, after DrVSP-mediated PIP_2 depletion, the shift of half-maximal activation voltage ($V_{0.5}$) was much smaller in E7K than WT, particularly around the physiological range of membrane potential (below +50 mV): $V_{0.5}$ values before and after VSP activation were 62.07 ± 7.32 and 83.31 ± 9.53 vs. 59.63 ± 10.79 and 219.84 ± 75.37 for E7K and WT, respectively (*n* = 8). Consequently, in the negative membrane potential range, WT channels were strongly suppressed after VSP-mediated PIP_2 depletion, whereas E7K channels were less affected (Figure 4A). These results indicate that the E7K mutant may remain functional even after vigorous depletion of endogenous PIP_2, possibly because of its tight binding to PIP_2. Being consistent with this possibility, an N-terminal polypeptide

carrying the E7K mutation tended to show a more potent binding to $PI(4,5)P_2$ than that of WT (Figure S1). These results provide an interesting explanation that tighter binding to (or interaction with) endogenous PIP_2 may strengthen the voltage-dependent activation of the E7K-TRPM4 channel.
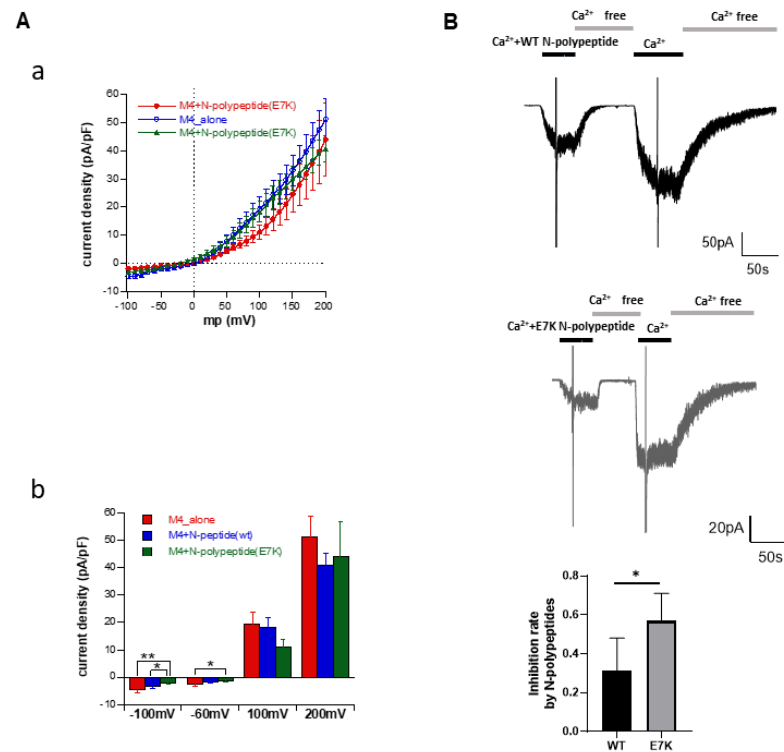

Figure 5. Different degrees of inhibition by WT- and E7K-N-terminal polypeptides of TRPM4 channels. (**A**) Current-voltage (I-V) relationships of full-length WT-TRPM4 channel co-expressed in HEK293 cells with either WT- or E7K-N-terminal polypeptides (the first 100 amino acid residues), or an empty vector alone (a). TRPM4 current was induced by 1 μM Ca^{2+} under the whole-cell conditions. The densities of inward and outward TRPM4 currents were compared at membrane potentials of −120, −60, 100, and 200 mV (b). The E7K polypeptide was more effective than WT polypeptide at inhibiting whole-cell TRPM4 currents. *: $p < 0.05$ with ANOVA followed by Tukey's post hoc tests ($n = 7$). Only the pairs of columns that show statistically significant differences are shown. (**B**) Direct application of short synthetic N-terminal polypeptides containing the 'WT' and 'E7K' sequences suppressed single-TRPM4 channel activities induced by 100 μM Ca^{2+} at −60 mV. Representative data from two inside-out patches showing greater inhibition by E7K- than WT polypeptides. *: $p < 0.05$ with unpaired *t*-test, respectively ($n = 5$).

3.5. N-Terminal Polypeptides Inhibit TRPM4 Channel Activity

The hitherto-mentioned results indicate that the 'E7K' sequence in the N-terminus may be critical for enhanced PIP_2 affinity and activity of the mutant TRPM4 channel. To substantiate this idea more directly, we created N-terminal polypeptides containing WT (EKE[5-7]) or E7K (EKK[5-7]) sequences and compared their inhibitory effects on TRPM4 channel activity. An empty vector (control) or that containing the first 100 N-terminal amino acid residues of either WT or E7K was co-expressed with the full-length WT-TRPM4 channel into the HEK293 cells. In the whole-cell configuration at a holding potential of −60 mV, intracellular perfusion of 1 μM Ca^{2+} via a patch electrode-elicited robust TRPM4 current was observed (not shown). The co-expression of either WT- or E7K polypeptides in the pipette significantly inhibited these currents, in particular around the resting membrane potential (Figure 5Aa). As summarized in Figure 5Ab, although both WT- and E7K polypeptides significantly reduced the density of the whole-cell inward TRPM4 current, the E7K polypeptide was more effective than the WT polypeptide (e.g., at −100 mV,

-3.23 ± 0.60 and -1.92 ± 0.43 pA/pF with WT- and E7K polypeptides, respectively, vs. -4.65 ± 0.78 pA/pF with an empty vector alone). Consistent with this observation, simultaneous application of shorter synthetic N-terminal polypeptides containing the WT and E7K sequences suppressed single-TRPM4 channel activities induced by 100 µM Ca^{2+} (top and middle panels in Figure 5B), but the degree of the inhibition was greater with E7K- than WT polypeptides (0.56 ± 0.02 vs. 0.31 ± 0.03, respectively, $n = 5$) (bottom graph in Figure 5B). These results could be interpreted to mean that the 'E7K' sequence in the polypeptide more effectively hinders the N-terminal domain of TRPM4 channel protein from interacting with membrane PIP_2.

4. Discussion

Membrane phospholipids serve as the structural foundation for intracellular signaling, which is most commonly initiated by receptor activation to alter a variety of ion channel/transporter activities. The PIP_2 turnover is tightly linked to and capable of influencing the electrical properties of cardiomyocyte. Thus, altered PIP_2 response of certain cardiac ion channels could cause arrhythmia.

In this study, our findings show that the E7K mutation is associated with an enhanced interaction of TRPM4 channels with PIP_2. This mutation has been identified in a few pedigrees of patients' families associated with progressive conduction blocks and sudden death. Altered SUMOylation for the E7K mutation is suggested to be a molecular mechanism accounting for increased cell-surface expression of the TRPM4 channel protein and its consequent activity, which did not accompany changes in its gating behavior [6]. However, our preliminary results hinted that in this TRPM4 mutant, single-channel gating is also affected [22]. This suggests the presence of an additional functional modification, in which altered PIP_2 interaction could be involved, since it has been reported to have a significant impact on the TRPM4 channel's behavior [12].

There are several basic residues assumed to contribute to TRPM4 channel–PIP_2 interaction. In addition to rigorous interaction between PIP_2 and the C-terminal residues of this channel [12], recent studies identified an N-terminal domain that interacts with PIP_2 to exert an important functional modification [23]. It has also been proven that PIP_2 interacts with CaM-binding domains on the distal N-terminus of the TRPM3 channel [24]. Moreover, based on crystal structure information [25], a recent study suggested that TRP channel function could be modulated through the N- and C-terminal interactions [26]. All these studies support the possibility that PIP_2 can interact with TRP channels via multiple domains/regions in a complex manner. In our experiments, PIP_2-binding assay as well as functional analyses with synthetic PIP_2 analogs, DrVSP-mediated PIP_2 depletion, and N-terminal polypeptides demonstrated that a few charged amino acids on the distal N-terminus may also be essential in some way for the functional regulation of the TRPM4 channel via PIP_2 interaction.

To gain more physiological insights about how endogenous PIP_2 modulates TRPM4 channel activity, we utilized the capability of DrVSP to control the endogenous PIP_2 level. More specifically, since DrVSP induces a graded PIP_2 depletion by varying the strength of membrane depolarization without involvement of other second messengers that might modulate TRPM4 currents, this intervention, when combined with a PIP_2-reporting FRET probe (i.e., the CFPmse-PHd/YFPmse-PHd pair), allowed us to quantitatively evaluate the TRPM4 channel interaction with endogenous PIP_2 level in situ. Using these new experimental approaches, a good correlation was observed between FRET changes induced by DrVSP activation and the extent of concomitant TRPM4 channel inhibition, and this enabled us to compare differences in the interaction with endogenous PIP_2 between WT- and E7K-TRPM4 channels. In our study, DrVSP-mediated PIP_2 depletion almost instantaneously occurred upon strong depolarization, while the recovery from the depletion likely reflected the resynthesis of PIP_2 in the membrane, which required a longer time course.

DrVSP-mediated PIP_2 depletion induced a clear rightward shift in the voltage dependence of the WT-TRPM4 channel (Figure 4B), while the shift was almost absent in

the E7K mutant, especially around the resting membrane potential. This means that the E7K mutation rendered TRPM4 channel almost insensitive to vigorous PIP_2 depletion. The large difference in voltage dependency, in particular around the resting membrane potential, would support a greater arrhythmogenic risk of the E7K mutation in the TRPM4 channel, in addition to its enhanced activity due to increased cell-surface expression [6]. The apparent potency of PIP_2 to modulate TRPM4 channel activity estimated from the functional analyses in Figure 3 indicates that the E7K mutant interacts more closely with PIP_2 than WT, but they were only slightly different from each other (K_d values: 0.97 vs. 1.06 μM), which corresponds to only ~0.1RT difference in free energy for PIP_2 binding (or interaction). A similarly small difference in PIP_2 dependence was observed between the reactivation curves of desensitized WT and E7K mutant channels by diC_8PIP_2 (K_d: 2.40 vs. 1.44 μM, respectively; equivalent to a free energy difference of ~0.5RT; Figure 1C). These small differences in PIP_2 dependence appear insufficient to account for the largely discrepant PIP_2 dependence of voltage-dependent activation curves observed for the WT and E7K channels (i.e., the shifts of the curves by PIP_2 depletion were 21 and 160 mV, respectively; Figure 4B). In principle, the closed-to-open transition of voltage-dependent channels can be governed by two terms of free energy change, i.e., the voltage-independent conformational energy increase that occurs in the absence of membrane potential and the voltage-dependent energy increase or electrical energy increase proportionate to the movement of gating charges [27]. However, the large values of the slope factor of 60-100mV, which did not differ much between the WT and E7K mutant or change before and after DrVSP-mediated PIP_2 depletion (see the Figure 4 legend), indicate that the effective number of gating charges involved in the voltage-dependent activation of the TRPM4 channel would be far less than one, which is much smaller than those of purely voltage-dependent channels [27]. Therefore, the observed shift of the voltage-dependent activation curve for WT-TRPM4 channels upon PIP_2 depletion (Figure 4) would most likely reflect the voltage-independent conformational energy decrease resulting from the release of PIP_2-mediated 'steric interactions' within the channel complex which are essential for its activity [28]. These interactions would be strongly tightened in the E7K mutant, and this may be the reason why vigorous, but not complete, PIP_2 depletion by DrVSP activation resulted in only a marginal decrease of E7K channel activity. At present, however, it remains entirely unclear what structural/mechanistic basis is involved therein, since the only known atomic structure of the TRPM4 channel is its 'closed' configuration, which lacks the detailed information about the most distal part of the N-terminus [29].

Finally, in order to seek the possible physiological/pathophysiological implications of the present findings, we performed single-cell action potential (AP) simulations with complex Ca^{2+} dynamics for WT- and E7K-mutant TRPM4 channels. As performed previously, we adopted the Luo–Rudy 2000 ventricular AP model incorporated with TRPM4-gating kinetics [19]. Alterations in the rate constants of opening and closing were estimated from those obtained in the absence and presence of 5μM diC_8PIP_2 (Figure S2). The results of the simulation indicated that PIP_2 depletion prevents the arrhythmic changes in AP that would otherwise occur when TRPM4 protein expression and/or channel activity is pathologically upregulated 5- to 6-fold. In stark contrast, the presence of an E7K mutation almost eliminates this preventive effect of PIP_2 depletion, and renders the channel much more excitable. During sustained neurohormonal stresses in which cardiomyocytes progressively undergo remodeling changes, the expression of the TRPM4 channel is expected to dramatically increase [30], and concomitantly, the PIP_2 metabolism would be largely compromised [11]. Therefore, it is conceivable that the mechanism described above may help to reduce the arrhythmogenic risk as a negative feedback to suppress the excessive activation of TRPM4 channels, which is presumably disrupted by the E7K mutation. Moreover, it is tempting to speculate that during the cardiac remodeling processes, the overactivation of TRPM4 could occur in the different regions of the heart including the conduction system (e.g., Purkinje fibers), where an abnormal depolarizing shift of the resting membrane potential due to excessive TRPM4 channel activity may not only slow or halt AP conduction as the result of

increased inactivation of voltage-dependent Na^+ channels, but might also cause fibrotic degeneration of Purkinje fibers that could lead to permanent conduction failures (see the Introduction Section). Further work is needed to verify this interpretation.

In summary, the present study revealed the physiological significance of TRPM4–PIP_2 interaction to maintain channel activity. By using FRET-based PIP_2 sensors in combination with voltage-sensing phosphatase (DrVSP) and patch clamping, we clearly demonstrated that the activity of the WT-TRPM4 channel is positively correlated with the endogenous PIP_2 level, which is abnormally strengthened in the E7K mutant through modulation of voltage-dependent gating. Such altered PIP_2 interaction may provide a novel pathogenic mechanism underlying TRPM4 channelopathies including arrhythmias.

Supplementary Materials: The following are available online at https://www.mdpi.com/article/10.3390/cells10050983/s1, Figure S1: Phosphoinositide-binding of n-terminal peptides from WT and E7K mutant assessed by dot-blot assays. Figure S2: E7K mutation abrogates the preventive effect of a PIP2 decrease against arrhythmogenicity because of excessive TRPM4 activity.

Institutional Review Board Statement: Not applicable.

Informed Consent Statement: Not applicable.

Data Availability Statement: The data described in this paper are available on request.

Conflicts of Interest: The authors declare no conflict of interest.

References

1. Wong, C.X.; Brown, A.; Lau, D.H.; Chugh, S.S.; Albert, C.M.; Kalman, J.M.; Sanders, P. Epidemiology of sudden cardiac death: Global and regional perspectives. *Heart Lung Circ.* **2019**, *28*, 6–14. [CrossRef]
2. Hof, T.; Chaigne, S.; Récalde, A.; Sallé, L.; Brette, F.; Guinamard, R. Transient receptor potential channels in cardiac health and disease. *Nat. Rev. Cardiol.* **2019**, *16*, 344–360. [CrossRef]
3. Inoue, R.; Jensen, L.J.; Shi, J.; Morita, H.; Nishida, M.; Honda, A.; Ito, Y. Transient receptor potential channels in cardiovascular function and disease. *Circ. Res.* **2006**, *99*, 119–131. [CrossRef]
4. Launay, P.; Fleig, A.; Perraud, A.-L.; Scharenberg, A.M.; Penner, R.; Kinet, J.-P. Trpm4 is a Ca^{2+}-activated nonselective cation channel mediating cell membrane depolarization. *Cell* **2002**, *109*, 397–407. [CrossRef]
5. Simard, C.; Sallé, L.; Rouet, R.; Guinamard, R. Transient receptor potential melastatin 4 inhibitor 9-phenanthrol abolishes arrhythmias induced by hypoxia and re-oxygenation in mouse ventricle. *Br. J. Pharmacol.* **2012**, *165*, 2354–2364. [CrossRef]
6. Kruse, M.; Schulze-Bahr, E.; Corfield, V.; Beckmann, A.; Stallmeyer, B.; Kurtbay, G.; Ohmert, I.; Schulze-Bahr, E.; Brink, P.; Pongs, O. Impaired endocytosis of the ion channel trpm4 is associated with human progressive familial heart block type i. *J. Clin. Investig.* **2009**, *119*, 2737–2744. [CrossRef] [PubMed]
7. Rezazadeh, S.; Duff, H.J. Genetic determinants of hereditary bradyarrhythmias: A contemporary review of a diverse group of disorders. *Can. J. Cardiol.* **2017**, *33*, 758–767. [CrossRef]
8. Rosenhouse-Dantsker, A.; Mehta, D.; Levitan, I. Regulation of ion channels by membrane lipids. *Compr. Physiol.* **2011**, *2*, 31–68.
9. Hilgemann, D.W.; Feng, S.; Nasuhoglu, C. The complex and intriguing lives of PIP_2 with ion channels and transporters. *Sci. STKE* **2001**, *2001*, re19. [CrossRef]

10. Barki-Harrington, L.; Luttrell, L.M.; Rockman, H.A. Dual inhibition of β-adrenergic and angiotensin ii receptors by a single antagonist: A functional role for receptor–receptor interaction in vivo. *Circulation* **2003**, *108*, 1611–1618. [CrossRef]

11. Tappia, P.S.; Liu, S.-Y.; Shatadal, S.; Takeda, N.; Dhalla, N.S.; Panagia, V. Changes in sarcolemmal plc isoenzymes in postinfarct congestive heart failure: Partial correction by imidapril. *Am. J. Physiol. Heart Circ. Physiol.* **1999**, *277*, H40–H49. [CrossRef]

12. Nilius, B.; Mahieu, F.; Prenen, J.; Janssens, A.; Owsianik, G.; Vennekens, R.; Voets, T. The Ca^{2+}-activated cation channel trpm4 is regulated by phosphatidylinositol 4, 5-biphosphate. *EMBO J.* **2006**, *25*, 467–478. [CrossRef] [PubMed]

13. Zhang, Z.; Okawa, H.; Wang, Y.; Liman, E.R. Phosphatidylinositol 4, 5-bisphosphate rescues trpm4 channels from desensitization. *J. Biol. Chem.* **2005**, *280*, 39185–39192. [CrossRef]

14. Murata, Y.; Iwasaki, H.; Sasaki, M.; Inaba, K.; Okamura, Y. Phosphoinositide phosphatase activity coupled to an intrinsic voltage sensor. *Nature* **2005**, *435*, 1239–1243. [CrossRef]

15. van der Wal, J.; Habets, R.; Várnai, P.; Balla, T.; Jalink, K. Monitoring agonist-induced phospholipase c activation in live cells by fluorescence resonance energy transfer. *J. Biol. Chem.* **2001**, *276*, 15337–15344. [CrossRef] [PubMed]

16. Itsuki, K.; Imai, Y.; Hase, H.; Okamura, Y.; Inoue, R.; Mori, M.X. PLC-mediated PI(4, 5) P_2 hydrolysis regulates activation and inactivation of trpc6/7 channels. *J. Gen. Physiol.* **2014**, *143*, 183–201. [CrossRef]

17. Inoue, R.; Okada, T.; Onoue, H.; Hara, Y.; Shimizu, S.; Naitoh, S.; Ito, Y.; Mori, Y. The transient receptor potential protein homologue trp6 is the essential component of vascular α1-adrenoceptor–activated Ca^{2+}-permeable cation channel. *Circ. Res.* **2001**, *88*, 325–332. [CrossRef] [PubMed]

18. Erickson, M.G.; Liang, H.; Mori, M.X.; Yue, D.T. Fret two-hybrid mapping reveals function and location of L-type Ca^{2+} channel cam preassociation. *Neuron* **2003**, *39*, 97–107. [CrossRef]

19. Hu, Y.; Duan, Y.; Takeuchi, A.; Hai-Kurahara, L.; Ichikawa, J.; Hiraishi, K.; Numata, T.; Ohara, H.; Iribe, G.; Nakaya, M. Uncovering the arrhythmogenic potential of trpm4 activation in atrial-derived HL-1 cells using novel recording and numerical approaches. *Cardiovasc. Res.* **2017**, *113*, 1243–1255. [CrossRef]

20. Falkenburger, B.H.; Jensen, J.B.; Hille, B. Kinetics of PIP_2 metabolism and kcnq2/3 channel regulation studied with a voltage-sensitive phosphatase in living cells. *J. Gen. Physiol.* **2010**, *135*, 99–114. [CrossRef] [PubMed]

21. Imai, Y.; Itsuki, K.; Okamura, Y.; Inoue, R.; Mori, M.X. A self-limiting regulation of vasoconstrictor-activated trpc3/c6/c7 channels coupled to PI(4, 5) P_2-diacylglycerol signalling. *J. Physiol.* **2012**, *590*, 1101–1119. [CrossRef]

22. Ishikawa, Y. The 95th annual meeting of the physiological society of Japan. *J. Physiol. Sci.* **2018**, *68*, 1–210. [CrossRef]

23. Bousova, K.; Jirku, M.; Bumba, L.; Bednarova, L.; Sulc, M.; Franek, M.; Vyklicky, L.; Vondrasek, J.; Teisinger, J. PIP_2 and PIP_3 interact with *n*-terminus region of trpm4 channel. *Biophys. Chem.* **2015**, *205*, 24–32. [CrossRef]

24. Holendova, B.; Grycova, L.; Jirku, M.; Teisinger, J. Ptdins (4, 5) P_2 interacts with cam binding domains on trpm3 *n*-terminus. *Channels* **2012**, *6*, 479–482. [CrossRef] [PubMed]

25. Autzen, H.E.; Myasnikov, A.G.; Campbell, M.G.; Asarnow, D.; Julius, D.; Cheng, Y. Structure of the human trpm4 ion channel in a lipid nanodisc. *Science* **2018**, *359*, 228–232. [CrossRef]

26. Zheng, W.; Cai, R.; Hofmann, L.; Nesin, V.; Hu, Q.; Long, W.; Fatehi, M.; Liu, X.; Hussein, S.; Kong, T. Direct binding between pre-s1 and trp-like domains in trpp channels mediates gating and functional regulation by PIP_2. *Cell Rep.* **2018**, *22*, 1560–1573. [CrossRef]

27. Hille, B. Ionic channels in excitable membranes. Current problems and biophysical approaches. *Biophys. J.* **1978**, *22*, 283–294. [CrossRef]

28. Thompson, M.J.; Baenziger, J.E. Ion channels as lipid sensors: From structures to mechanisms. *Nat. Chem. Biol.* **2020**, *16*, 1331–1342. [CrossRef]

29. Duan, J.; Li, Z.; Li, J.; Santa-Cruz, A.; Sanchez-Martinez, S.; Zhang, J.; Clapham, D.E. Structure of full-length human trpm4. *Proc. Natl. Acad. Sci. USA* **2018**, *115*, 2377–2382. [CrossRef] [PubMed]

30. Guinamard, R.; Demion, M.; Magaud, C.; Potreau, D.; Bois, P. Functional expression of the trpm4 cationic current in ventricular cardiomyocytes from spontaneously hypertensive rats. *Hypertension* **2006**, *48*, 587–594. [CrossRef]